Journal of Fluorine Chemistry 134 (2012) 11–17

Contents lists available at ScienceDirect

Journal of Fluorine Chemistry

journal homepage: www.elsevier.com/locate/fluor

Review

Applicative performances of fluorinated carbons through fluorination routes: A review

Katia Guérin *, Marc Dubois, Axel Houdayer, André Hamwi

Clermont-Université, Laboratoire des Matériaux Inorganiques, UMR CNRS 6002-Université Blaise Pascal, 24 av. des Landais, 63171 Aubière Cedex, France

ARTICLE INFO

Article history:
Received 20 January 2011
Received in revised form 10 June 2011
Accepted 16 June 2011
Available online 23 June 2011

Keywords:
Nanocarbons
Direct fluorination
Catalytic fluorination
Fluorination by fluorinating agent
Carbon fluorides
Primary lithium battery

ABSTRACT

Electrochemical performances of fluorinated carbons and nanocarbons as electrode materials for primary lithium batteries are reviewed and compared with the ones of conventional carbon fluorides. Fluorination conditions strongly influence the electrochemical performances, then different strategies of fluorination have been developed, by the group "Fluorination and fluorinated materials" of the laboratory of Inorganic Materials in Clermont University, in order to promote some particular electrochemical parameters, namely the discharge potential, the energy density, the power density or the faradic yield. As a consequence, 3 new ways of fluorination have been carried out since 10 years in our laboratory: (i) catalytic fluorination combined with a post fluorination under pure fluorine gas, (ii) sub-fluorination process and (iii) fluorination by TbF_4, XeF_2, ... decomposition. Enhanced electrochemical performances have been obtained and the fluorination mechanisms of each family of fluorinated carbons have been better understood thank to a deep physico-chemical characterization by XRD, IR and Raman spectroscopies, solid state NMR with ^{13}C and ^{19}F nuclei and EPR.

Contents

1. Introduction

Lithium primary batteries are commonly used for many applications such as cameras, electrical lock, electronic counter, electronic measurement equipment, emergency power source, memory back-up, spatial, military and implantable medical devices. All these applications require power sources with high energy densities, good reliability, safety and long life. One of the attractive chemistries is that provided with a fluorine based cathode and more particularly carbon fluoride (denoted as CF_x). Generally, solid carbon fluorides are prepared by direct reaction of fluorine gas with carbonaceous materials (conventional fluorination). A temperature higher than 350 °C is needed if graphite or graphitized carbon materials (for example, petroleum coke heat treated at 2800 °C) are used [1–3]. The higher the reaction temperature, the higher the fluorination level x (x = F:C, $0.5 < x < 1$) of compounds (then called

* Corresponding author. Tel.: +33 473407567; fax: +33 473407108.
E-mail address: katia.guerin@univ-bpclermont.fr (K. Guérin).

0022-1139/$ – see front matter © 2011 Elsevier B.V. All rights reserved.
doi:10.1016/j.jfluchem.2011.06.013

$(CF)_n$) and the higher the C–F covalent character, where the carbon atoms are in sp^3 hybridization. Nevertheless, because of the decomposition reaction of CF_x (whatever the x value), the fluorination temperature must not exceed 600 °C, at which the x value reaches one for graphite as starting material. When amorphous or disordered (less graphitized) carbons (petroleum coke, carbon black, active carbon, ...) [4,5] are used as starting materials, the fluorination level x exceeds sometimes one fluorine atom per carbon atom indicating the formation of CF_2 and CF_3 groups. These latter should be less active than C–F groups because C–F bond energies in $>CF_2$ and $-CF_3$ are higher and then the specific faradic capacity decreases. For such kind of disordered materials, different processes compete: (i) fluorination with C–F bond formation, (ii) perfluorination with CF_2 and CF_3 formation on the sheet edges and defects, and even, (iii) decomposition, for which volatile carbon fluorides are evolved. Therefore, graphite (natural or artificial) and highly graphitized carbon (coke or others high temperature heat treated) used as starting materials are more suitable because of the easier control of the reaction.

Actually, in the Li/CF_x battery system, a high oxidation–reduction potential of the cathode reaction is combined with low weight density of light C and F elements. The use of CF_x materials as the active cathode in primary lithium batteries was first demonstrated by Watanabe and Fukuda [6] and then a few years later, the first Li/CF_1 batteries were commercialised by Matsushita Electric Co. in Japan [7]. Commercial Li/CF_x batteries consists in a coke based cathode having a F:C molar ratio equal or slightly higher than unity. The main features of the Li/CF_1 batteries are: high energy density (up to 1560 Wh kg^{-1}), high average operating voltage (around 2.4 V vs. Li^+/Li), long shelf life (higher than 10 years at room temperature), stable operation and wide operating temperatures (−40 °C/170 °C).

Up to now the energy density of carbon fluorides is high because of mainly a high discharge capacity. Indeed, the average discharge potential is significantly lower than the theoretical electrochemical potential for a pure ionic C–F bond calculated in between 4.5 and 5 V vs. Li^+/Li. Only new fluorination ways can allow an increase of the average discharge potential as well as others electrochemical parameters which are deficient such as the power density or the faradic yield. With such aims, our strategy focuses around the fluorination conditions in order to enlarge the applicative markets of carbon fluorides; for example, space applications require higher operating temperature ranges, higher current densities and higher power densities. Indeed, due to kinetic limitations associated with the poor electrical conductivity of strongly covalent CF_1 material, the battery can sustain only low to medium range discharge currents. As for the faradic yield, most of the time it does not exceed 75% because of too high amounts of inactive CF_2 and CF_3 groups and dangling bonds which are considered as structural defects and hinder the lithium diffusion.

For average discharge potential increase, many researchers have focused on catalytic fluorination which allows to enhance fluorine reactivity and therefore to be able to use lower reaction temperatures. The lower the fluorination temperature, the lower the C–F bonding energy is. When minute amounts of a volatile fluoride such as HF, AsF_5, IF_5, OsF_6, WF_6, SbF_5, and so on, [8,9] were introduced into the fluorine atmosphere. Fluorinated graphites were thereby obtained from ambient temperature up to 100 °C. All these compounds exhibit a fluorination level x = F:C lower than 0.5, with C–F bonding either ionic (weak bonding energies, $x < 0.25$) or semi-ionic (or semi-covalent) involving stronger bonding energies: $0.25 < x < 0.5$, but less than that corresponding to covalent ones. Moreover, it has been shown that, whatever the fluorine content, sp^2 carbon hybridization (i.e. planarity of graphene layers) is maintained despite the fluorine intercalation reaction into graphite [9,10]. High increase of discharge potential has been obtained but, up to now, such materials are not industrialized because of both a low discharge capacity and some discharge capacity loss during ageing. However, during long storage of the primary lithium battery some residual intercalated species, which are always present in a few amounts because of the fluorination mechanisms, are removed from the fluorographite inter-layers and dramatically disturb the electrochemical processes. To our knowledge, very few investigations have been focused on low power densities and faradic yield of carbon fluorides so far.

In this paper, we will show the strategies developed to (i) enhance the energy density by an increase of the average discharge potential, (ii) improve both the power density and the faradic yield. For each purpose, new fluorination processes are needed: catalytic fluorination combined with a post fluorination under pure fluorine gas for higher energy density [11–21], sub-fluorination process for higher power density [22–26] and fluorination by fluoride decomposition (fluorinating agents) for higher faradic yield [27–29]. Among the various solid fluorinating agents, terbium tetrafluoride TbF_4 has been chosen. New enhanced electrochemical performances such as power density of 8000 W kg^{-1} have been obtained and fluorination mechanism for each family of fluorinated carbon has been better understood thank to a deep physico-chemical characterization by X-ray diffraction (XRD), infrared and Raman spectroscopies, solid state NMR with both ^{13}C and ^{19}F nuclei and electron paramagnetic resonance EPR.

2. How to increase energy density?

2.1. Catalytic fluorination combined with post-direct fluorination

At room temperature, the reactivity of fluorine gas with graphite is greatly improved by the presence of a volatile fluoride and anhydrous HF gaseous mixture [10]. Most efficient volatile fluorides MF_n were: ClF_3, BF_3, IF_5, BrF_5, ReF_6, WF_6, MoF_6. First stage highly fluorinated graphite compounds of formula $CF_x(M_y)$, with $0.5 < x < 0.9$ and $0.06 < y < 0.02$, were obtained. The obtained x value depends on the used fluoride MF_n because the fluorination level is related to the Lewis acidity of the volatile fluoride and its interaction with HF. It seems that the higher values correspond to the lower Lewis acidity of fluoride relative to that of HF [30]. The highest degree of fluorination was then achieved using IF_5 which is considered as a slightly weaker Lewis acid than HF. Fluorinated graphites were prepared using Madagascar natural graphite powder (particle size of 7.5 μm) at room temperature thanks to synthesis methods which were already described [11]. Graphite reacts with a gaseous mixture of fluorine (F_2), hydrogen fluoride (HF) and volatile inorganic fluoride (IF_5). The fluorinated graphites thus obtained were called CF_x-IF_5. The fluorination levels have been estimated by considering the weight uptake. In order to both improve the fluorination level and to remove the residual catalyst, this compound was subjected to a heat treatment under a stream of pure fluorine gas at a temperature (T_{PF}) ranging between 150 and 680 °C during 3 h. The resulting compounds prepared are denoted CF_x-IF_5-T_{PF}.

It has been found that iodine fluoride residues are progressively de-intercalated from the structure and that they play a key role on the peculiarity of these materials. Three types of materials have been generated according to the post-treatment temperature (see Scheme 1) [11]:

- for post-fluorination temperatures lower than 400 °C, the C–F bond is mainly weakened covalent but the fluorographite compounds contain some residual catalysts,
- for post-fluorination temperatures comprised between 400 °C and 550 °C, the C–F bonding became more and more covalent, because of both an increase of the fluorine amount in the

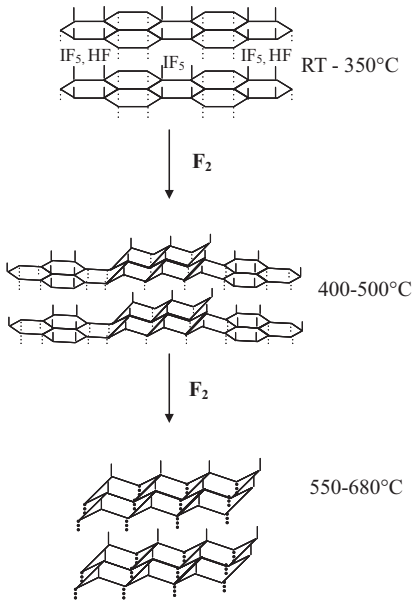

Scheme 1. Post-fluorination mechanism of low temperature fluorinated graphite.

carbonaceous matrix and the progressive de-intercalation of the residual catalysts (no more residual catalysts remain trapped into the fluorographene layers),

- for higher post-fluorination temperatures (between 550 and 680 °C), physicochemical characteristics of obtained compounds and conventional high temperature graphite fluorides (prepared by direct fluorination of graphite at about 600 °C) were surprisingly different (see Section 2.2) in spite of a similar fluorination rate and a pure covalent C–F bond. The progressive conversion of both the carbon hybridization from sp^2 to sp^3 and the C–F bonding, allows low structural defects to be obtained. Such difference results in interesting electrochemical performances.

2.2. Post-fluorination treatment influenced on the energy density

Fluorinated carbon samples were studied as cathode in primary lithium batteries. Composite electrodes were made of fluorinated carbon sample (about 80% by weight, w/w), graphite powder (10%, w/w) to insure electronic conductivity and polyvinylidene difluoride (PVDF, 10%, w/w) as binder. The mass of active material was between 2 and 10 mg for all the experiments. A two electrodes cell was used (Swagelok cell type), where lithium was both reference and counter electrode. A PVDF microporous film wet with electrolyte composed of a lithium salt ($LiClO_4$) dissolved in PC (doubly distilled) with 1 mol L^{-1} concentration, was sandwiched between the composite electrode and a lithium metal foil. The cells were assembled in an argon filled dried glove box. Relaxation was performed for at least 5 h until open cell voltage (OCV) stabilization. Galvanostatic discharges were performed at room temperature between the initial OCV and 1.5 V with a VMP2 –Z under current densities ranged between 10 and 720 A kg^{-1}. The capacity Q_{exp} was measured with a potential cut-off of 2.0 V. The average discharge potential $E_{1/2}$ corresponds to the potential obtained at half of the total discharge.

These 3 types of materials lead to singular electrochemical behaviour [12]. It must be noted that the fluorination range of these 3 types are different than the fluorination range discussed above because as we will see now the amount of residual catalyst species is the key parameter and not the carbon hybrization change as it was before.

- For fluorination post-treatment temperatures included between 100 °C and 300 °C, both average discharge voltage and capacity remain constant, around 3.0 V vs. Li^+/Li and 570 Ah kg^{-1}, respectively. Again, the high discharge voltage results from the weakened covalence of the C–F bond. The energy density, shown in Fig. 1, increases with the capacity and is already, for these fluorination post-treatment temperatures, higher than the one of conventional carbon fluorides. This energy density value is the result of high average discharge potential of 3.0 V and low discharge capacity of about 570 Ah kg^{-1}.
- For post-treatment temperatures between 300 and 550 °C, a low decrease of the discharge potential [from 3 to 2.53 V] occurs concomitantly with a high increase of the discharge capacity [570–900 Ah kg^{-1}]. This results in a progressive increase with the post-fluorination temperature of the energy density, which rises up to 2277 Wh kg^{-1}. The decrease of the average discharge potential is explained mainly by the change of C–F bonding toward a more covalent character whereas the increase of the capacity correlates with the removal of iodine fluoride species and the concomitant increase of fluorine content with post-fluorination treatment. The energy density is particularly high for the graphite fluoride compounds (post-fluorination temperature between 400 and 500 °C) where the two carbon hybridization states (i.e. sp^2 and sp^3) co-exist; this seems to favor very good electrochemical performances.
- For a fluorination post-treatment temperature higher than 550 °C, both the average discharge voltage (as expected due to changes in C–F bonding) and the discharge capacity decrease. As in the case of conventional carbon fluorides, the increase of inactive CF_2 and CF_3 groups identified by FT-IR and ^{19}F NMR measurements and hindering dangling bonds (paramagnetic and thus detected by EPR) explain the lowering of the capacity. However, despite a similar fluorination temperature (600 °C), post-treated low temperature graphite fluorides yields noteworthy higher energy density than conventional carbon fluorides in good accordance with the low amounts of structural defect when compared to conventional graphite fluorides.

The post-treated low temperature graphite fluoride materials offer a wide range of (voltage, capacity) characteristics suitable for specific battery operating requirements. Tuning the fluorination post-treatment temperature is the key parameter in achieving such a specific material. The co-existence of sp^2 and sp^3 hybridized

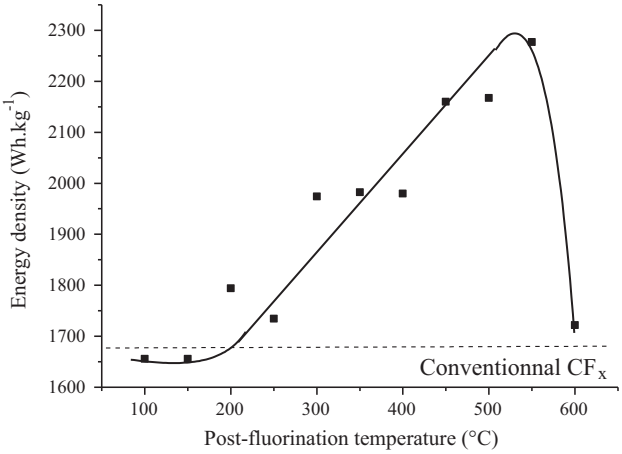

Fig. 1. Evolution of energy density as a function of post-fluorination temperature for low temperature fluorinated graphite.

carbons with varying sp^2/sp^3 ratios result in varying C–F bond strength from weakened covalent to covalent. A maximum of 2277 Wh kg^{-1} of energy density is obtained for a post-fluorination temperature of 500 °C and as these compounds do not contain traces of IF_y catalysts, no altering of the cell's shelf-life should occur. Such materials are suitable for industrial applications.

3. How to increase the power density?

3.1. Sub-fluorination process of carbon nanofibres

The low power density of carbon fluorides is due to the association of kinetic limitations and the poor electrical conductivity of strongly covalent $(CF)_n$ material. To increase this electrochemical performance, our approach consists in the enhancement of the intrinsic electrical conductivity of CF_x cathode materials thanks to the control of the kinetics conditions for carbon fluorination. A process, called sub-fluorination, has then been applied on carbons. The best results have been obtained with carbon nanofibres CNFs as precursors. Indeed, their one dimension texture allows the nanostructuration of the fluorinated carbonaceous matrix.

High purity (>90%) carbon nanofibres (CNFs) which are 8–20 mm in diameter with 2–20 μm lengths have been supplied by MER corporation, they have been obtained by CVD method and then post-treated under argon atmosphere at 1800 °C. Fluorinated carbon nanofibres (CNFFs) were prepared with 200 mg of CNFs at temperatures T_T ranging between 380 °C and 480 °C in F_2 atmosphere for a reaction time of 16 h. The sub-fluorination process consists in combining a minute control of the fluorination conditions, i.e. temperature T_T, fluorine gas flow rate (g min^{-1}) and time [24]. One main characteristic of this new family of materials is the presence of nano-domains of unfluorinated carbon atoms in the core of the nanomaterials which facilitate the electron flow within the particles (Fig. 2). The targeted composition 'x' $0.2 < x < \sim 1.0$ have been achieved. The fluorination level 'x' (i.e. F:C molar ratio) of CNFFs was determined by gravimetry (weight uptake) and by quantitative ^{19}F NMR measurements. ^{19}F and ^{13}C Magic Angle Spinning (MAS) (14 and 10 kHz spinning rates, respectively) NMR experiments were carried out at room temperature on a Bruker AVANCE DSX 300 spectrometer operating at 282.36 and 75.47 MHz, respectively. For ^{19}F NMR the external reference was CF_3COOH. All the ^{19}F chemical shifts are referenced to $CFCl_3$ ($\delta_{CF_3COOH} = -78.5$ *vs.* $CFCl_3$). For ^{13}C NMR the external reference was tetramethylsilane (TMS).

Because of the nanostructuration of the fibres, which can be described as multi-walled carbon nanotubes with large diameter, and of its post-treatment graphitization, the fluorination temperature T_F is higher than the one needed for graphite in pure 1 atm. F_2 gas. Such nanostructuration needs a progressive fluorination which processes from the outer tubes of the nanocarbon toward its core (supported by SEM and TEM images). In fact, four fluorination temperature zones can be pointed out for sub-fluorinated carbon nanofibres, denoted CNFFs [22]:

For T_F ranged in between 435 and 450 °C, interesting CNFFs with a nearly constant $x \sim 0.7$–0.8 were obtained. The fluorine atoms have progressed from the outer walls toward the core forming a $(C_2F)_n$ type carbon fluoride structure ('stage-2' compound with FCCF slabs stacking sequence) of the fluorinated part. Unfluorinated domains are still present as clearly evidenced by ^{13}C NMR analysis. For higher fluorination temperatures $(C_2F)_n$ phase is irreversibly converted into $(CF)_n$-type one ('stage-1' compound with FCF slabs stacking sequence) and this conversion leads unfortunately to some exfoliation.

Accordingly, for $435 < T_F < 450$ °C, the fluorinated domains, which are the electrochemically active parts of the cathode material are intermixed at nano-scale with unfluorinated domains, which insure the electron flow in the electrochemical processes. This last point plays a key role in enhancing the intrinsic electrical conductivity of the CNFFs materials and is the origin of the high energy density, as discussed in the following part.

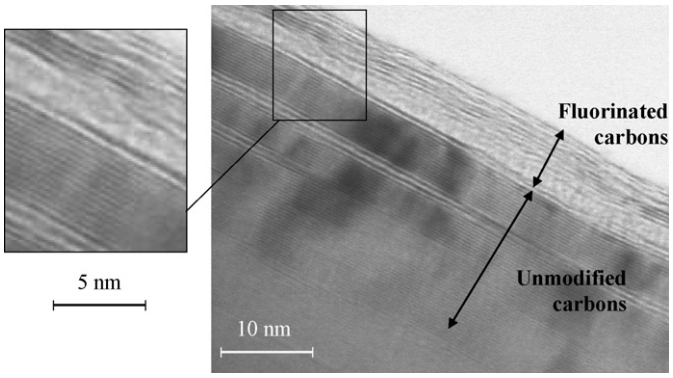

Fig. 2. TEM bright field images of carbon nanofibres sub-fluorinated at 420 °C.

3.2. Electrochemical properties

Whatever the samples, at low discharge current density, the average discharge potential is set in a very narrow range (2.45–2.6 V) [23,24]. This quasi stability is in agreement with the covalent C–F bonding which does not change upon fluorination. Although the discharge voltage and the fluorine content of CNFFs are close to those reported in $(C_2F)_n$-type graphite fluoride, the achieved discharge capacity of the CNFFs materials synthesized between 435 and 450 °C is about 30% higher than those of $(C_2F)_n$. Moreover, an impressive 8057 W kg^{-1} power density associated with a high 1749 Wh kg^{-1} energy density were achieved in CNFFs with F:C equal to 0.76 (obtained both by quantitative NMR and by gravimetry), whose galvanostatic discharge is presented in Fig. 3. Here, the power density is 6 times higher than the one of conventional graphite fluorides. Then, for $F:C > 0.80$, the maximum power density decreases but is still higher than the one of conventional graphite fluorides. Such high and new performances are due to the presence of non-fluorinated carbons in the CNFFs core with a percentage higher than 10%, which favors fast electron flow and accordingly enhances the electrode reaction kinetics [23]. Actually, the effect of enhanced conductivity is more pronounced at higher discharge rates at which the power density difference of the new materials with conventional CF_1 becomes obvious. In fact, whatever the CNFFs cathode material, including a lightly fluorinated $CF_{0.21}$ (obtained both by quantitative NMR and by gravimetry), both the achieved C-rate and the power density are higher than for CF_1. That is why such process is now developed by Contour Energy System society (licensed patent [24]). Industrial fabrication using the sub-fluorination process started 2 years ago and will increase according to the market.

4. How to increase the faradic yield of carbon fluorides?

4.1. Fluorination by TbF_4 decomposition

One interesting research is to focus on the decrease of the level of perfluorinated groups such as CF_2, CF_3 and dangling bonds which are inactive electrochemical and/or limit the lithium/fluorine diffusion. Such perfluorination can be weakened by the choice of an alternative reactive species such as atomic fluorine $F^\bullet$ instead of molecular fluorine F_2. Its higher diffusivity and reactivity could favor the formation of C–F bond. For this purpose, fluorination

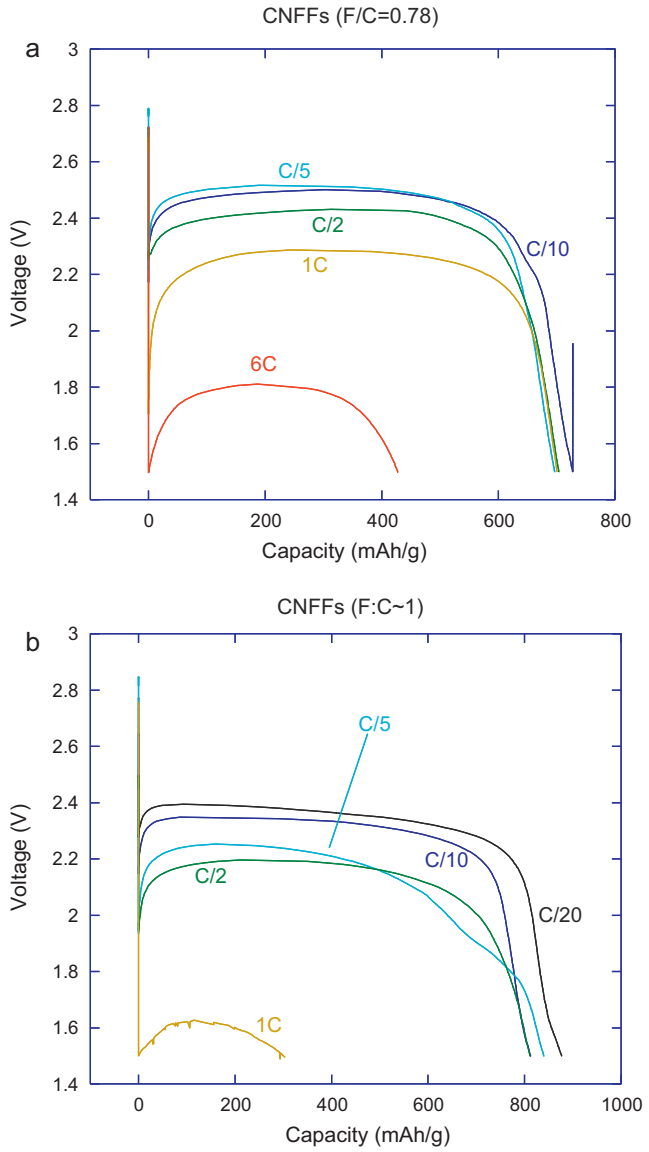

Fig. 3. Galvanostatic discharge curves for different current densities of carbon nanofibres sub-fluorinated at 450 °C (a) compared to the ones of conventional $(CF)_n$ with F:C = 1 (b).

process called fluorination by TbF_4 decomposition was developed. TbF_4 powder was obtained from TbF_3 (Aldrich, 99.9%) fluorination in pure F_2 gas at 500 °C. Its purity (i.e. the absence of residual TbF_3) was systematically checked by X-ray diffraction. The thermogravimetric analysis (TGA) of freshly prepared TbF_4 indicated that exactly one mole of $F^\bullet$ was released per mole of TbF_4 between 300 and 500 °C. For the CNFs fluorination by TbF_4, a nickel closed reactor was used in order to preserve the defined fluorine amount released by the thermal decomposition of TbF_4. A two temperatures oven was used: the part containing TbF_4 was heated at 450°C whatever the experiment whereas CNFs were heated at temperatures T_F ranged between 420 and 500 °C. A reaction time of 16 h was used. Prior to the heating, a primary vacuum ($\sim 10^{-2}$ atm) was applied into the reactor. The reactions involved during the fluorination are the following:

$$TbF_4 \xrightarrow{\Delta} TbF_3 + F^\bullet \quad \text{or} \quad \frac{1}{2}F_2$$

$$C + xF^\bullet \quad \text{or} \quad \frac{x}{2}F_2 \rightarrow CF_x$$

The total conversion of TbF_4 into TbF_3 was systematically checked by both the weight loss and the X-ray diffraction analysis.

TbF_4 decomposition at temperatures around 450 °C releases exactly 1 mole of pure atomic fluorine per 1 mole of initial TbF_4, which recombines with carbon and more particularly CNFs. As the reactive species are different between sub-fluorination and fluorination, the fluorination mechanisms differ. During the way with TbF_4, because the fluorine amount is by the equilibria $TbF_4(s) \Leftrightarrow TbF_3(s) + F^\circ$ and $2F^\circ(g) \Leftrightarrow F_2(g)$, the fluorination is more progressive and homogeneous leading to the formation of $(CF)_n$-type phase whatever the fluorination conditions, i.e. the highly fluorinated phase. No $(C_2F)_n$-type phase is formed as in the case of sub-fluorination or more generally for direct process with graphitized starting materials. During this process, with increasing T_F a progressive densification of the $(CF)_n$-type compound takes place and very few amounts of CF_2, CF_3 and dangling bonds are formed as shown in Fig. 4. Room temperature ^{19}F MAS NMR (14 kHz) is well adapted to underline the relative amount of CF_2 and CF_3 groups, which exhibit chemical shifts of −60/−90 and ∼−120 ppm vs. $CFCl_3$, respectively. The spectra of two representative samples with similar fluorine content ($x \sim 0.6$) from direct and fluorination by TbF_4 decomposition are shown in Fig. 4. The lines related to CF_2 and CF_3 groups are less intense for the sample obtained with TbF_4. Such an observation can be done whatever the fluorine content. The CF_3 groups, can be localized on the fluorocarbon sheet edges and probably possess a spinning motion around the C–C bonds, explaining the narrowness of the resonance line. Moreover, the ^{19}F MAS NMR spectra of CNFs fluorinated by TbF_4 decomposition and direct processes exhibit similar isotropic line located at −190 ppm/$CFCl_3$. This latter is attributed to fluorine atoms covalently bonded to carbon atoms (C–F) [14,21,31,32]. The similarities of the main isotropic line reveal the same C–F bonding whatever both the fluorination way and the temperature. Nevertheless, another difference between the fluorinated carbon nanomaterials obtained using the two routes exists: first, the presence of a line at −178 ppm for intermediate fluorination temperature by the direct process and another at −120 ppm also for the direct fluorination. The line at −178 ppm appears only for fluorinated carbons which contain fluorinated parts with a $(C_2F)_n$ structure and can be attributed to fluorine atoms bonded with non-fluorinated sp^3 carbon atom itself bonded with another sp^3 carbon

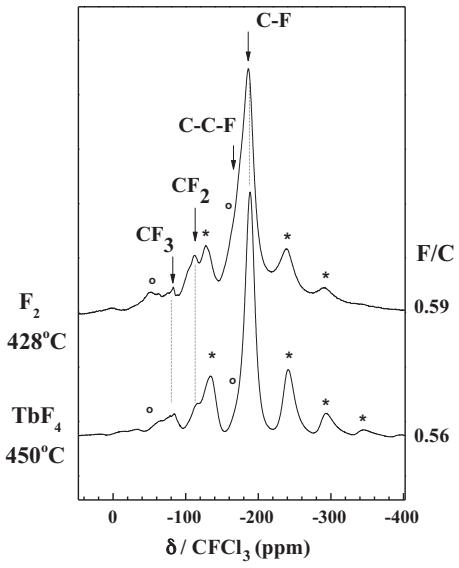

Fig. 4. Solid state ^{19}F MAS NMR spectra (14 kHz) of fluorinated carbons with close fluorine content (F:C ∼ 0.6) obtained by direct (428 °C) and TbF_4 (450 °C) processes; * and ○ mark spinning sidebands.

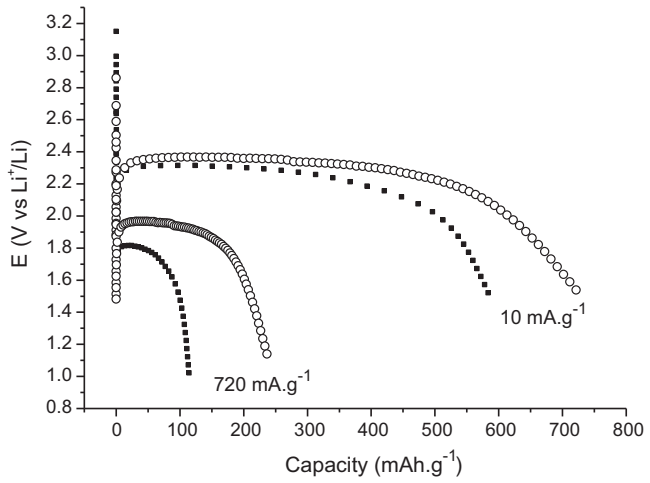

Fig. 5. Galvanostatic discharges curves at 10 mA g^{-1} (C/100) and at 720 mA g^{-1} (1C) for CNFs with F:C ~ 0.70 fluorinated either with direct process (■) or TbF_4 ones (○).

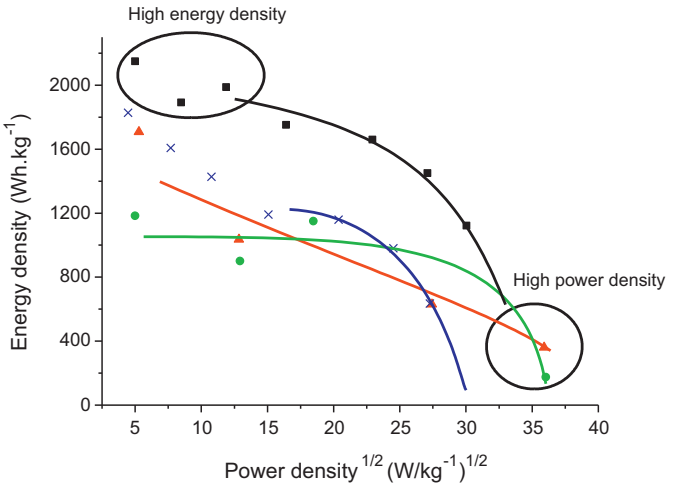

Fig. 6. Ragone plot of fluorinated carbons (graphite or carbon nanofibres as precursors) with fluorine level of about 0.7 obtained by catalytic fluorination + post direct fluorination (■), sub-fluorination (●) and fluorination by solid fluorinating agent (▲) compared to values for conventional product (×) [14,24].

atom in accordance with the $(C_2F)_n$ structure. Another defect, dangling bonds, have been found using EPR to be present in less amounts after fluorination by TbF_4 decomposition whatever the fluorine content. Finally, according to transmission electron microscopy images, the fluorinated parts are homogenously dispersed in the carbon matrix using TbF_4 as fluorinating agent contrary to the sample obtained using F_2, where only the outer tubes are fluorinated for low and medium *x* ratio [26,27].

4.2. Electrochemical properties

In order to compare the electrochemical performances of fluorinated CNFs obtained by TbF_4 and direct fluorination, materials with similar fluorine level have been used as cathode in primary lithium batteries. We will focus on *x* of about 0.7–0.8 because of its good performances. Different current densities have been applied to the two materials and Fig. 5 presents the discharge curves for the extreme current densities i.e. 10 mA g^{-1} and 720 mA g^{-1} corresponding at C/100 and 1C, respectively. Whatever the electrochemical conditions, both the potential and the capacity are higher for CF_x prepared by TbF_4 way by comparison with direct process and it results in faradic yield close to 100% for materials prepared by fluorination by TbF_4 decomposition. The low increase of potential cannot be explained by a variation of the covalence of the C–F bonding as we already mentioned that solid state NMR has revealed exactly the same C–F bonding whatever the fluorination way. It can be explained by a lowering of internal resistive effect such as lithium or fluorine barrier diffusion due to CF_2, CF_3 type groups located at the edges of the fluorinated compounds or dangling bonds. The higher the amount of such groups, the higher internal resistance is. The higher capacity of compound prepared by fluorination using TbF_4 decomposition can also be explained by an indirect contribution of CF_2 or CF_3 type groups. Indeed, they contribute to the fluorine level value which is used to the prediction of the theoretical capacity. But as they cannot be reduced, the true active mass is actually overestimated like the capacities.

5. Conclusions

In order to avoid the failures such as power density, faradic yield and energy density of fluorinated carbon materials used as electrode in primary lithium battery, 3 new fluorination ways have been developed allowing the performances of carbon fluorides to be significantly enhanced (Table 1 and Fig. 6). The highest energy density of 2300 Wh kg^{-1} has been obtained thanks to the room temperature catalytic process followed by a post fluorination treatment at 450 °C over graphite, the highest power density of 8000 W kg^{-1} associated with high current densities (6C) for sub-fluorination applied on one-dimension nanocarbons and the highest faradic yield for fluorination by TbF_4 decomposition. The last decade of investigations underlines that the nanostructuration of the allotropic forms of carbon and the development of new fluorination ways, optimized for such kind of materials, are two key parameters which would generate higher electrochemical performances of carbon fluorides, in particular in terms of average discharge potential. As matter of fact, a weakening of the C–F bonding results from a curvature of the raw carbon lattice [33]. The electroreduction could occur at higher potential with interesting benefits in terms of power density and management of heating

Table 1
Summary of the electrochemical performances of carbon fluorides as a function of the fluorination way.

	Raw carbon	Q_{exp} (mAh g^{-1})	$E_{1/2}$ (V)	Energy density (Wh kg^{-1})	Current density	Power density (W kg^{-1})
Conventional product	Coke	800	2.1	1680	1C	1370
Sub-fluorination	CNFs	800	2.4	1920	6C	>8000
Catalytic fluorination + post-fluorination	Graphite	900[a]	3.15[b]	2300[b]	C/2	1200
Fluorination using TbF_4	CNFs	809	2.4	1900	5C	6500

Q_{exp}: experimental capacity.
[a] Post-treatment at 550 °C.
[b] Post-treatment at 150 °C.
Q_{exp}, $E_{1/2}$, Energy density data obtained at low current densities (C/100).
Power density obtained for the highest current density available.

effects. Although the use of fluorinated materials as electrode materials is known since many years, new applications would be found taking into account the enhanced performances. Our laboratory keeps on conducting researches to further optimize these performances of these fascinating materials.

Acknowledgments

The authors wish to express theirs thanks to Pr. F. Masin (Université Libre de BRUXELLES, U.L.B. BELGIUM), Dr. R. Yazami (INPG, LEPMI, St. MARTIN D'HERES, FRANCE), Dr. Z. Fawal (Université Libanaise, Faculté des Sciences III, TRIPOLI, LIBAN), Dr. J. P. Pinheiro, W. Zhang, C. Delabarre, J. Giraudet, for their cooperation in this work and our fruitful discussions.

References

[1] N. Watanabe, T. Nakajima, H. Touhara, Graphite Fluorides, Elsevier, Amsterdam, 1988
[2] T. Nakajima, N. Watanabe, Graphite Fluorides and Carbon–Fluorine Compounds, CRC Press, Boston, 1991.
[3] A. Hamwi, K. Guérin, M. Dubois, Fluorinated Materials for Energy Conversion, Elsevier, Oxford, UK, 2005.
[4] N. Watanabe, R. Hagiwara, T. Nakajima, J. Electrochem. Soc. 131 (1984) 1980–1984.
[5] A. Morita, N. Eda, T. Ijima, H. Ogawa, in: J. Thompson (Ed.), Power Sources, 9, Academic Press, New York, 1983, p. 435.
[6] N. Watanabe, M. Fukuda, US Patent 3,536,532 (1970) and 3,700,502 (1972).
[7] M. Fukuda, T. Iijima, in: D.H. Collins (Ed.), Power Sources, 5, Academic Press, New York, 1975, p. 713.
[8] I. Palchan, D. Davidov, H. Selig, J. Chem. Soc. Chem. Commun. 12 (1983) 657.
[9] T. Nakajima, N. Watanabe, I. Kameda, M. Endo, Carbon 24 (1986) 343–351.
[10] A. Hamwi, M. Daoud, J.C. Cousseins, Synth. Met. 26 (1988) 89–98.
[11] K. Guérin, J.P. Pinheiro, M. Dubois, Z. Fawal, F. Masin, R. Yazami, A. Hamwi, Chem. Mater. 16 (2004) 1786–1792.
[12] K. Guérin, R. Yazami, A. Hamwi, Electrochem. Solid State Lett. 7 (6) (2004) A159–A162.
[13] M. Dubois, K. Guérin, J.P. Pinheiro, F. Masin, Z. Fawal, A. Hamwi, Carbon 42 (10) (2004) 1931–1940.
[14] J. Giraudet, M. Dubois, K. Guérin, J.P. Pinheiro, A. Hamwi, W.E.E. Stone, P. Pirotte, F. Masin, J. Solid State Chem. 178 (2005) 1262–1268.
[15] C. Delabarre, K. Guérin, M. Dubois, J. Giraudet, Z. Fawal, A. Hamwi, J. Fluorine Chem. 126/7 (2005) 1078–1087.
[16] J. Giraudet, C. Delabarre, K. Guérin, M. Dubois, F. Masin, A. Hamwi, J. Power Sources 158 (2) (2006) 1365–1372.
[17] C. Delabarre, J. Giraudet, K. Guérin, M. Dubois, A. Hamwi, J. Phys. Chem. Solids 67 (5–6) (2006) 1157–1161.
[18] K. Guérin, M. Dubois, A. Hamwi, J. Phys. Chem. Solids 67 (5–6) (2006) 1173–1177.
[19] C. Delabarre, M. Dubois, J. Giraudet, K. Guérin, A. Hamwi, Carbon 44 (12) (2006) 2543–2548.
[20] C. Delabarre, M. Dubois, J. Giraudet, K. Guérin, R. Yazami, A. Hamwi, ECS Transactions – Cancun 3 (36) (2007) 153–163.
[21] J. Giraudet, M. Dubois, K. Guérin, C. Delabarre, A. Hamwi, F. Masin, J. Phys. Chem. B 111 (51) (2007) 14143–14151.
[22] F. Chamssedine, M. Dubois, K. Guérin, J. Giraudet, F. Masin, D.A. Ivanov, L. Vidal, R. Yazami, A. Hamwi, Chem. Mater. 19 (2) (2007) 161–172.
[23] R. Yazami, A. Hamwi, K. Guérin, Y. Ozawa, M. Dubois, J. Giraudet, F. Masin, Electrochem. Commun. 9 (2007) 1850–1855.
[24] R. Yazami, A. Hamwi, WO2007098478 (2007), WO2007126436 (2007) and EP1999812 (2008), EP1976792 (2008).;
J. Whitacre, R. Yazami, R. Bugga, S. Prakash, M. Smart, W. West, A. Hamwi, WO2007098369 (2007) and EP1992028 (2008).
[25] W. Zhang, M. Dubois, K. Guérin, A. Hamwi, J. Giraudet, F. Masin, J. Solid State Chem. 181 (8) (2008) 1915–1924.
[26] W. Zhang, L. Moch, M. Dubois, K. Guérin, A. Hamwi, J. Nanosci. Nanotech. 9 (2009) 4496–4501.
[27] W. Zhang, K. Guérin, M. Dubois, Z. Fawal, D. Ivanov, L. Vidal, A. Hamwi, Carbon 46 (7) (2008) 1010–1016.
[28] W. Zhang, K. Guérin, M. Dubois, A. Houdayer, F. Masin, A. Hamwi, Carbon 46 (7) (2008) 1017–1024.
[29] W. Zhang, M. Dubois, K. Guérin, P. Bonnet, H. Kharbache, F. Masin, P. Thomas, J.-L. Mansot, A. Hamwi, Eur. Phys. J. B 75 (2010) 133–139.
[30] A. Hamwi, J. Phys. Chem. Solids 57 (1996) 677–688.
[31] H. Touhara, F. Okino, Carbon 38 (2000) 241–267.
[32] M. Panich, Synth. Met. 100 (1999) 169–185.
[33] W. Zhang, M. Dubois, K. Guérin, P. Bonnet, D. Claves, H. Kharbache, F. Masin, A.P. Kharitonov, A. Hamwi, Phys. Chem. Chem. Phys. 12 (2010) 1388–1398.